

THE INFLUENCE OF PASSIVE, LEADING EDGE TUBERCLES ON WING PERFORMANCE

P. Watts

Applied Fluids Engineering, Inc.

Private Mail Box #237, 5710 E. 7th Street, Long Beach, CA, 90803
phil.watts@appliedfluids.com

F. E. Fish

West Chester University

Department of Biology, West Chester, PA, 19383
ffish@wcupa.edu

Abstract

Tubercles on the leading edges of humpback whale flippers enhance maneuverability during prey capture. Tubercles may therefore be functional adaptations. By extension, leading edge modifications of streamlined bodies apparently offer cost-effective performance enhancements, including a passive means of increasing vehicle maneuverability. We have developed an efficient panel method simulation applicable to wings that move immersed in a fluid at large Reynolds numbers. The numerical simulation is used to evaluate the forces acting on the wing. When acting on a control surface, these forces govern maneuverability. We compare lift and drag forces for a wing with leading edge tubercles versus the same wing without tubercles at a 10° angle of attack. We find a 4.8% increase in lift, a 10.9% reduction in induced drag, and a 17.6% increase in lift to drag ratio. Tubercles enhance wing performance at modest angles of attack while offering no detrimental effects at zero angle of attack. We evaluate viscous drag forces acting on the wing and show that tubercles may incur an 11% increase in form drag at a 10° angle of attack. Tubercles may also extend the operational envelope of a control surface by delaying the onset and severity of stall. Consequently, the maximum force of a control surface may be substantially increased.

Introduction

Maneuvers made by vertebrate swimmers are often superior to those of engineered vehicles (Bandyopadhyay *et al.*, 1997). Part of this superiority can be attributed to the flexibility and control afforded by a spinal column surrounded by muscle. However, some of the benefits may also be attributed to the shape of aquatic animals. Biomimicry introduces new shapes into engineering design that may otherwise go untested. Selected shapes may offer a passive means of increasing maneuverability and stealth. We show that leading edge modifications of streamlined bodies can offer performance enhancements.

In many engineering applications, the leading edges of bluff and streamlined bodies are straight, presumably for historical reasons related to manufacturing methods. As is well known in the fluid dynamic literature, relatively small modifications near a leading edge

can substantially alter, delay or reduce separation effects (White, 1991). For wings, this is most often achieved by protrusions such as vortex generators that enhance boundary layer attachment. Yet, bluff bodies with sinusoidal upstream faces can experience a 30% reduction in drag (Bearman and Owen, 1998) and suppression of vortex shedding (Owen et al., 2000) without any lateral protrusions. These findings apply to bluff bodies with wavy separation lines where wave steepness is less than 10%. We demonstrate a proof of the concept that a mildly wavy leading edge can also enhance wing performance at a positive angle of attack.

Humpback Whale Flipper

Humpback whale flippers are remarkable in many ways, including their curved planform, large aspect ratio, and surprising articulation, especially when compared with other whale species (Edel and Winn, 1978). Humpback whale flippers also display leading edge tubercles, essentially leading edge bumps facing into the free stream flow, that alter the fluid flow over these wings (Benke, 1993). Humpback whales are the only cetaceans with tubercles, and the only baleen whales that rely on maneuverability to capture prey (Fish and Battle, 1995). Specifically, humpback whales use their flippers to achieve tight circles while rounding up and eating prey (Fish, 1999). Bushnell and Moore (1991) contemplated the possibility that tubercles could be functional adaptations, thereby imparting an advantage in maneuverability and prey capture. Humpback whale flippers closely resemble the 21% thick, low drag NACA 634-021 wing in cross section (Fish and Battle, 1995). We employ a single wing shape and standard engineering techniques to investigate changes in performance brought about by the addition of tubercles along the leading edge. We hope to motivate more detailed analyses of passive leading edge modifications on wing performance.

Inviscid Simulations

Fluid dynamic forces are needed to relate marine vehicle maneuvers to the performance of control appendages. We employ a 3D panel method code based on a first order vortex method (Hess, 1974; Katz and Plotkin, 1991). Three nodes form the vertices of a triangular panel, with line vortices connecting the nodes along the triangle perimeter. A collocation point is located at the centroid of each triangular panel. For fluid dynamic simulations, each solid body is tiled with panels having unknown vortex strengths. The vorticity of each panel influences the fluid velocity at every collocation point. The fluid velocity is linearly related to the vortex strength of each panel multiplied by a shape factor that is a function of panel geometry and collocation point position. Enforcing the no flow condition into the body at each collocation point provides a system of linear equations for the unknown panel vortex strengths. Solving the system of equations by inverting the influence matrix yields the fluid flow outside of the body at a given instant of time. Most programming and computational effort is dedicated to matrix inversion.

The advantages of a panel method are significant. Surface distributions of fluid dynamic singularities (i.e., vortices) are ideally suited for high Reynolds number flows where boundary layers are thin (Hess, 1974). Fluid flow is calculated based on a surface

distribution of panels rather than a volumetric distribution of cells, lowering the computational cost of obtaining a highly accurate solution. This reduction in computational order is accomplished with the exact 3D Greens function of a vortex filament. Boundary layers are readily introduced by displacing panels away from the body surface (Katz and Plotkin, 1991). Wakes and fluid separation are readily simulated by introducing free vortices into the flow (Sarpkaya, 1989). Moreover, vortex filaments naturally reproduce shear layers and turbulent flows in ways that volume-based simulation methods still have difficulty accomplishing. The disadvantages of a panel method are more subtle. The singular nature of the Greens function around a vortex core can induce unrealistically large wake motions and oscillations in neighboring body panel vorticity. Hence, solution accuracy can actually increase by using larger panels and time steps, contrary to most numerical methods. We use regularization to suppress the singularity and smooth the solution results (Howle, 1999). Similarly, the positioning and strength of free vortices at separation require rules of thumb (Sarpkaya, 1989). Nevertheless, panel methods retain significant predictive power and global accuracy even though the initial mathematical elegance is lost in the details of implementation.

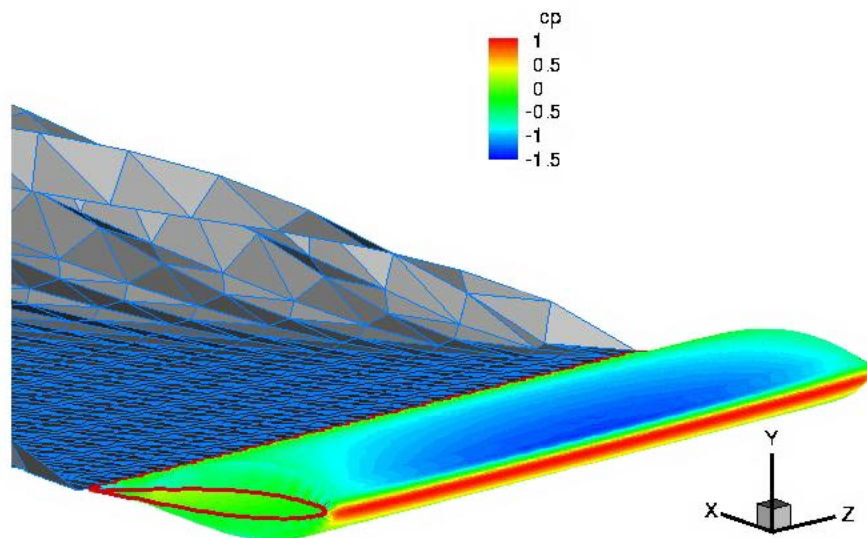


Figure 1 Simulation of flow over a finite span wing with straight leading edge

To begin with, we validated the panel method code by simulating inviscid fluid flow around a circular cylinder, a problem for which there is an exact analytical solution. We then validated lift *versus* angle of attack for the finite wing under consideration here, by combining 2D measurements (Abbott and von Doenhoff, 1959) with basic airfoil theory

on the effect of finite aspect ratio (Anderson, 1991). Similarly, we compared our chordwise pressure profile with experimental and simulated results and found excellent agreement. Fig. 1 shows the nondimensional pressure coefficient over the surface of a wing at a 10° angle of attack using a false color scheme. Low static pressures along the top of the wing (blue) generate lift but taper off towards the wing tips and towards the trailing edge. The stagnation region is displayed as a red line just underneath the leading edge of the wing. For this simulation, the chord is $c=0.176$ m, and the span is $b=0.359$ m, for an aspect ratio of 2.04. The airfoil is moving at $U_0=1$ m/s, and the timestep used was $dt=0.6$ s.

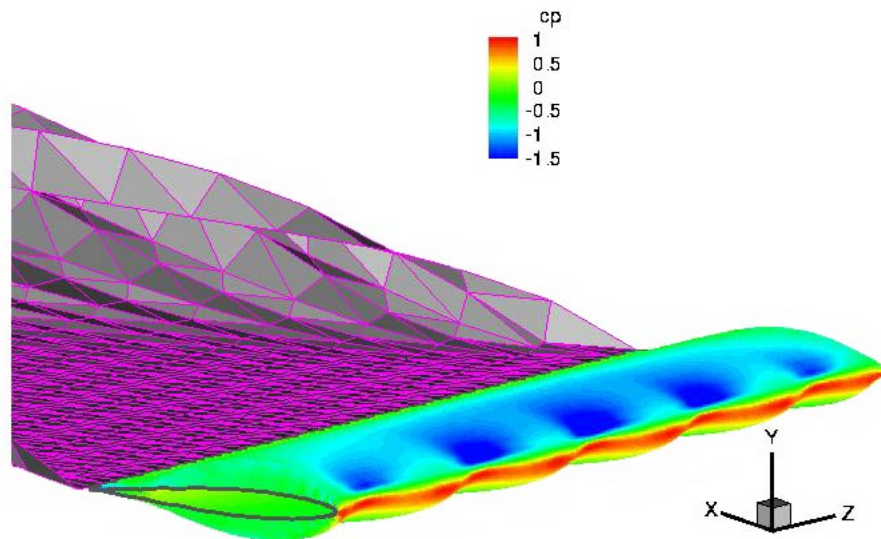


Figure 2 Simulation of flow over a finite span wing with leading edge tubercles

Fig. 2 provides a false color image of the nondimensional pressure coefficient over the surface of a wing at a 10° angle of attack, this time with tubercles along the leading edge. Reasonably broad low pressure regions reside between tubercles as indicated by the dark blue color. The leading edge shows significant variations in the intensity of the red line. The same color scheme is used in both figures. For a straight leading edge, we obtain $C_l=0.435$, and $C_{di}=0.0562$, while for the wing with tubercles we calculate $C_l=0.456$, and $C_{di}=0.0501$. The theoretical lift coefficient for this wing at this angle of attack is about 0.45. In sum, we find a 4.8% increase in lift, a 10.9% reduction in induced drag, and a 17.6% increase in lift to drag ratio when compared with the wing shown in Fig. 1. The planform area change due to tubercle protrusion is zero because the sinusoidal variations were made about the leading edge, as opposed to being added to the leading edge.

Viscous Calculations

We calculated boundary layer growth and mean viscous drag for the wing with and without tubercles. We chose the two end members of entirely laminar and entirely turbulent boundary layers as characteristic quantities of interest. We employ the Karman momentum integral relation to evaluate boundary layer development and shear stress subject to an imposed flow velocity outside of the boundary layer, which we obtain from the panel method simulation. For laminar boundary layers, we employ the method of Thwaites; whereas, for turbulent boundary layers, we employ correlations of turbulent parameters (White, 1991). We curve fit the chordwise velocity profiles obtained from our inviscid simulation with

$$\frac{u(y)}{U_o} = \sqrt{1 - C_p} = \frac{k_1 + k_2 y + k_3 y^2}{k_4 + k_5 y + k_6 y^2} \quad (1)$$

to r^2 values greater than 0.9986, where $y=x/c$ is zero at the leading edge and increases along the nondimensional chord, and C_p is the pressure coefficient shown in the previous two figures. These approximate techniques yield shear stresses accurate to within about $\pm 10\%$ under most applications, including boundary layers along wings. They can also locate separation points given an accurate velocity profile.

For unit chord $c=1$ and unit free stream velocity $U_o=1$, the total shear stress per unit width from both sides of the wing without tubercles is $\tau_t=2.07$ Pa for a laminar boundary and $\tau_t=2.55$ Pa for a turbulent boundary layer. By integrating spanwise along one complete tubercle, we find total shear stress per unit width of $\tau_t=2.31$ Pa for a laminar boundary layer and $\tau_t=2.82$ Pa for a turbulent boundary layer. These total shear stress values differ somewhat from flat plate solutions because of stagnation point displacement thicknesses and chordwise pressure gradients. For the two wings studied here, turbulent boundary layers have about 20% more shear stress than laminar boundary layers, regardless of leading edge shape. The shear stress of the wing with tubercles is 11% greater for both laminar and viscous boundary layers, which is barely above the resolution of the simulation technique (White, 1991). The trough between tubercles experiences 10% higher total shear stress than most other spanwise locations. The drag per unit width of the wing is the total shear stress multiplied by the chord. Neglecting separation near the trailing edge, we calculate a wing drag coefficient of around $C_d=0.005$, which is close to the measured value for small angles of attack (Abbott and von Doenhoff, 1959).

Discussion

The increase in lift attributed to the tubercles follows directly from the loss of a stagnation line along the leading edge (Fig. 3). In an inviscid simulation, leading edge suction is responsible for rotating the aerodynamic force to a vertical orientation, because there can be no form drag by assumption (Anderson, 1991). Any increase in leading edge suction, as we have documented here, would tend to rotate the lift vector past vertical and towards the oncoming flow. Because this is not possible in a steady, inviscid simulation

without sources of vorticity, the increase in leading edge suction must also be accompanied by an increase in wing lift. Alternatively, the lift can be integrated from the pressure coefficient over the surface of the wing. In this parallel explanation, the increased lift of the wing with tubercles arises from higher pressure along the bottom surface, rather than any noteworthy change in mean pressure along the top surface. The center of lift is pushed back by the low pressure plateau located behind the troughs, as seen by comparing Figs. 1 and 2. The net effect is a shift in pressure gradients without a significant net shift in mean pressure along the top surface.

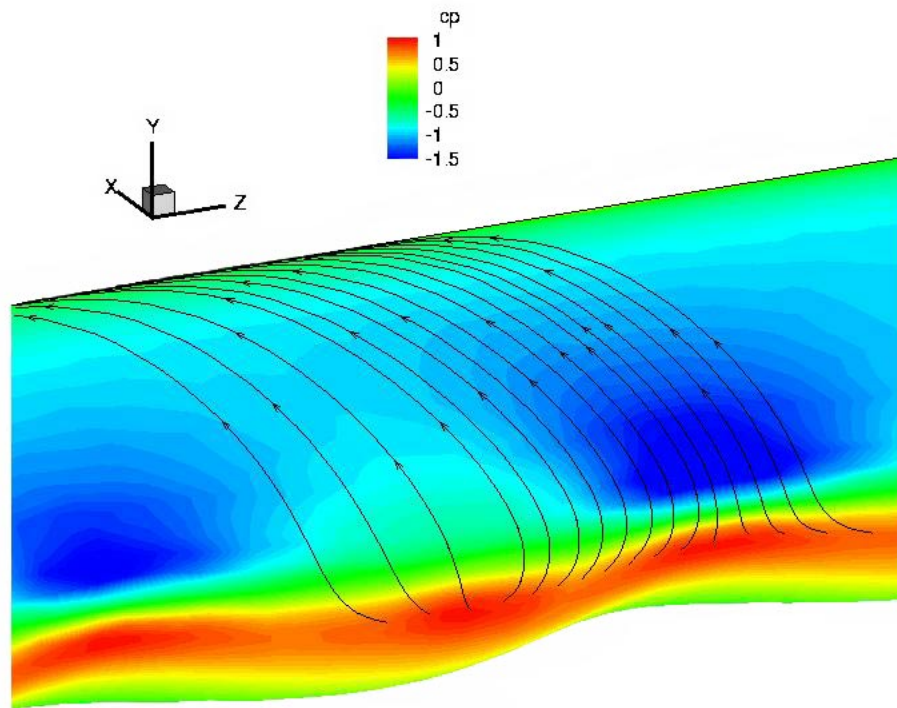


Figure 3 Streamlines outside of the boundary layer yet near the surface

There is very little variation in shear stress along the upper surface of wings with and without tubercles. The adverse pressure gradient starting near the quarter chord position and extending to the trailing edge induces relatively little shear stress as the boundary layer thickens and separation is approached, but not quite reached. Separation is commonly defined by a vanishing friction coefficient (White, 1991) and usually begins at the trailing edge of a wing (Anderson, 1991). The larger shear stress associated with the tubercles is imparted primarily by the favorable pressure gradient that extends along almost all of the bottom wing surface. The favorable pressure gradient suppresses boundary layer growth, thereby increasing shear stress. For a wing with tubercles, the favorable pressure gradient is enabled by a pressure coefficient of $C_p \approx -0.5$ at the trailing

edge, instead of $C_p \approx 0.5$ without tubercles. We consider our results as characteristic values because we did not model 3D boundary layers with streamwise vorticity (White, 1991). The large majority of the inviscid flow in Fig. 3 is aligned along the chord. Also, changes in the location of transition from a laminar to a turbulent boundary layer as well as separation of the boundary layer may be more important determinants of total shear stress than the two scalar values provided here.

The reduction in induced drag is probably due to the compartmentalization of lift between the troughs. The spanwise distribution of lift in a typical wing is usually dominated by wing tip vortices, planform, twist, etc. These are wing descriptors that either influence or are defined over the entire wing span. In contrast, tubercles generate a perturbation of the spanwise distribution of lift that is a local fluid dynamic response situated near the trough. The consequence is a reduction in the strength of the wing tip vortices while at the same time achieving enhanced lift. It could be said that the wing tip vortex is no longer a consequence of the entire wing, but rather a response to the tubercle closest to the wing tip. Induced drag is inversely proportional to wing aspect ratio. Therefore, our work is most relevant to smaller aspect ratio control surfaces commonly found on aquatic vertebrates and marine vehicles.

Conclusions

Tubercles appear to be functional adaptations of humpback whale flippers. Leading edge shape modifications such as tubercles can increase useful force production while simultaneously reducing parasitic forces. Few other passive means of altering fluid flow around a wing can both increase lift and reduce drag at the same time. The idea of appropriating tubercles from humpback whales for engineering purposes is a direct consequence of biomimicry. The performance enhancement that we document for 10° angle of attack vanishes as the angle of attack decreases to zero, implying no penalty for the presence of tubercles during a null state. A study of characteristic viscous forces revealed an increase in form drag comparable to the savings in induced drag at 10° angle of attack. We will study changes in tubercle spacing and shape to see if further enhancement is possible at the same angle of attack. However, the greatest potential gains can be made at angles of attack greater than 15° , where boundary layer separation and wing stall can be expected. Wavy separation lines on bluff bodies support the hypothesis, yet to be confirmed experimentally, that tubercles may alter, delay, or reduce separation at higher angles of attack. Boundary layer control techniques such as vortex generators that delay wing stall often increase maximum lift by 30% or more. Optimal control of maneuvering vehicles usually consists of maximal deflection of control surfaces. Streamlined bodies such as fins and rudders may experience larger control forces and extended operating envelopes due to the addition of leading edge tubercles. The ability to reduce wing tip vorticity suggests that tubercles could also enhance the stealth of marine vehicles.

Acknowledgments

Shaun Shariff developed the panel method code. John Long and Rob Root encouraged the early stages of the research. This work is supported by the Office of Naval Research under contract N00014-00-C-0341.

References

- Abbot, I. H. and von Doenhoff, A. E. (1959). Theory of wing sections. Dover.
- Anderson, J. D. (1991). Fundamentals of aerodynamics. McGraw-Hill.
- Bandyopadhyay, P. R., Castano, J. M., Rice, J. Q., Philips, R. B., Nedderman, W. H. and Macy, W. K. (1997). Low-speed maneuvering hydrodynamics of fish and small underwater vehicles. *Trans. ASME* **119**, 136-144.
- Bearman, P. W. and Owen, J. C. (1998). Reduction of bluff-body drag and suppression of the vortex shedding by the introduction of wavy separation lines. *J. Fluids and Structures* **12**, 123-130.
- Benke, H. (1993). Investigations on the osteology and the functional morphology of the flipper of whales and dolphins (Cetacea). *Invest. Cetacea* **24**, 9-252.
- Bushnell, D. M. and Moore, K. J. (1991). Drag reduction in nature. *Ann. Rev. Fluid Mech.* **23**, 65-79.
- Edel, R. K. and Winn, H. E. (1978). Observations on underwater locomotion and flipper movement of the humpback whale *Megaptera novaeangliae*. *Mar. Biol.* **48**, 279-287.
- Hess, J. L. (1974). The problem of three-dimensional lifting potential flow and its solution by means of surface singularity distributions. *Computer Methods in Appl. Mech. and Engineering* **4**, 283-319.
- Howle, L. E. (1999). Undulatory flap propulsion. Proc. 11th Int'l. Symp. Unmanned Untethered Submersible Technology (UUST), Autonomous Undersea Systems Institute, Durham, NH.
- Katz, J. and Plotkin, A. (1991). Low-speed aerodynamics. McGraw-Hill.
- Fish, F. E. and Battle, J. M. (1995). Hydrodynamic design of the humpback whale flipper. *J. Morphology* **225**, pp. 51-60.
- Fish, F. E. (1999). Performance constraints on the maneuverability of flexible and rigid biological systems. Proc. 11th Int'l. Symp. Unmanned Untethered Submersible Technology (UUST), Autonomous Undersea Systems Institute, Durham, NH.

Owen, J. C., Szewczyk, A. A. and Bearman, P. W. (2000). Suppression of Karman vortex shedding. *Phys. Fluids* **12(9)**, 9.

Sarpkaya, T. (1989). Computational methods with vortices: The 1988 Freeman Scholar lecture. *J. Fluids Engineering* **111**, pp. 5-52.

White, F. M. (1991). *Viscous fluid flow*. McGraw-Hill.